Extended Abstracts of the 2003 International Conference on Solid State Devices and Materials, Tokyo, 2003, pp. 330-331

E-6-4

Analytical SPICE Modeling of Realistic MOS-based Single-Electron Transistors –"MOSETs" with a Unique Distribution Function in the Coulomb Oscillation Region

Kyung Rok Kim*, Ki-Whan Song, Gwanghyeon Baek, Hyun Ho Kim, Jung Im Huh, Jong Duk Lee, Byung Gook Park
Inter-University Semiconductor Research Center, School of Electrical Engineering, Seoul Nat'l Univ.,
San 56-1, Shinlim-dong, Kwanak-gu, Seoul, 151-742
Phone: 82-2-880-7279, FAX: 82-2-882-4658, *e-mail: rocky@smdl.snu.ac.kr

1. Introduction

In recent researches, there have been strong efforts to observe single-electron charging effects in the conventional metal-oxide-semiconductor field effect transistor (MOSFET) structure without any additional electrode for the tunneling barriers [1,2]. To utilize these single-electron charging effects as a practical operation principle in single-electron transistors (SETs) based on MOSFETs, clear formation mechanism of quantum dot and tunnel barrier should be guaranteed and the MOSFET current needs to be sufficiently smaller than the Coulomb oscillation current for reliable high temperature operation.

In this paper, novel MOS-based SETs –"MOSETs" using band-to-band tunneling in the junctions are demonstrated and their electrical characteristics are analyzed by SPICE model with analytic equations based on the unique device physics.

2. Device Structure and Electrical Characteristics

MOSETs fabricated on a SIMOX (separation by implanted oxygen) *p*-type (100) wafer are schematically shown in Fig. 1 (a). The key process is the ion implantation of channel dopants up to degenerate doping level, which is larger than the effective density of state ($N_V \sim 1.04 \times 10^{19}/\mathrm{cm}^3$) in the silicon valence band. Consequently, MOSET has the available empty states in the valence band of the square channel region [3]. Figure 1 (b) shows the energy band diagram of MOSET at thermal equilibrium state. Under these conditions, degenerate p^+-n^+ tunnel barriers and the 30-nm square channel act as tunneling barriers and a Si island in SET, respectively. In addition, it can be noted that the tunneling current will flow only for a certain range of gate voltages and the conventional MOSFET current will take over, depending on the surface potentials controlled by the gate voltage (V_{GS}). As shown in Fig. 2, electrical characteristics of the fabricated MOSET at 77 K indicate the existence of Coulomb oscillations in the subthreshold region. Therefore, the equivalent circuit model of MOSET for the SPICE simulation should be represented by the parallel connection of SET and MOSFET (Inset of Fig. 2) and the total current of MOSET (I_{MOSET}) should be the superposition of SET current (I_{SET}) and the inherent MOSFET current (I_{MOS}) : $I_{MOSET} = I_{SET} + I_{MOS}$.

3. Implementation of the Analytical SPICE Model

A. SET current (I_{SET})

The intrinsic SET current ($I_{i\text{-}SET}$) equation for I_{SET} was based on the SET circuit model with the analytical equations [4,5], which have the gate, source, and drain capacitance as the elementary model parameters. These parameters can be extracted from the contour plot in Fig. 3 by extracting the oscillation period and slopes of the Coulomb diamond at low drain bias region. From these capacitances, the phase shift (ΔV_{GS}) due to drain voltage (V_{DS}) is $0.6V_{DS}$, which has the consistency with ΔV_{GS} of the second peak for each V_{DS} in the measured characteristics of Fig. 4. However, there are some discrepancies between the simulation and experimental results around the first and third peak of the oscillations especially at high V_{DS}.

To describe these exceptional turn-on and turn-off characteristics of Coulomb oscillations, a distribution function in the analytical considerations of the energy band structure should be incorporated into I_{SET}. This function can be written as :

$$f_D(V_{th}, V_p, m) = \frac{1}{1+\exp\left(\dfrac{(V_{th}-V_p)-V_G}{mk_BT}\right)} \times \frac{1}{1+\exp\left(\dfrac{V_G-V_{th}}{mk_BT}\right)} \quad (1)$$

where V_{th} is threshold voltage of inherent MOSFET, V_p is degeneracy factor and, m is the *body-effect coefficient*. Figure 5 (a) shows the shape of f_D with estimated parameters from the experimental conditions. This equation based on the Fermi-Dirac distribution function imply that I_{SET} can be observed even though $V_G > V_{th}$ as in the measured *I-V* characteristics. When this distribution function is incorporated into I_{SET} as : $I_{SET} = I_{i\text{-}SET} \times f_D$, the simulation results (lines) show good agreement with the measured *I-V* (symbols) around the first peak current even at relatively high V_{DS} (Fig. 5 (b)).

B. Inherent MOSFET current (I_{MOS})

The primary MOSFET current in the Coulomb oscillation region is the subthreshold current as: $I_{MOS} \sim \exp[(V_G - V_{th})/mk_BT]$. From the estimated subthreshold swing of 170 mV/dec at 77 K, *body-effect coefficient m* is about 10, which is consistent with the value used in the distribution function f_D and this value is reasonable considering heavy channel doping concentrations and relatively thick gate dielectric. Figure 6 (a) shows that the second peak and valley currents come to reach the measured values by adding subthreshold current and it should be noted that there is no significant increase in the first peak and valley currents, which are separated from the inherent MOSFET current. The complete SPICE simulation results of MOSETs including the linear MOSFET current region are shown in Fig. 6(b).

4. Conclusions

We have implemented an analytical SPICE model of realistic MOSET incorporating a unique distribution function. SPICE simulation of our model has reproduced the experimental results with good agreement at wide gate and drain bias range and thus, we have validated the operation principle of MOSET by the physics-based analytic equations.

Acknowledgements

This work has been supported by the BK21 Program and "Development of Nanoelectronic Devices and Circuit Technology" from Korean Ministry of Commerce, Industry, and Energy.

References

[1] M. Sanquer. et. al, *Phys. Rev. B* 61, 11, 7249 (2000)
[2] F. Boeuf et al., *Tech. Dig. of 2001 IEDM*, p. 29.5.1
[3] K. R. Kim et. al, *IEEE Electron Device Lett*., 23 612 (2002)
[4] K. Uchida et al., *Jpn. J. Appl. Phys*. 39, 2321 (2000)
[5] S.-H. Lee et al., *IEEE Trans. Nanotechnology* 1, 226 (2002)

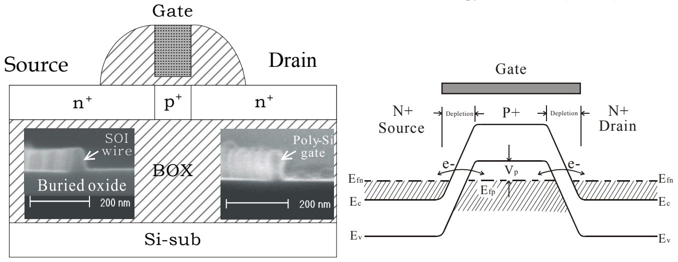

(a) (b)

Fig. 1. (a) Cross-sectional schematic of the fabricated "MOSET". Inset shows the SEM images of 30-nm-wide SOI channel and poly-Si gate, respectively. (b) Schematic energy band diagram of MOSET under the gate along the channel at thermal equilibrium state.

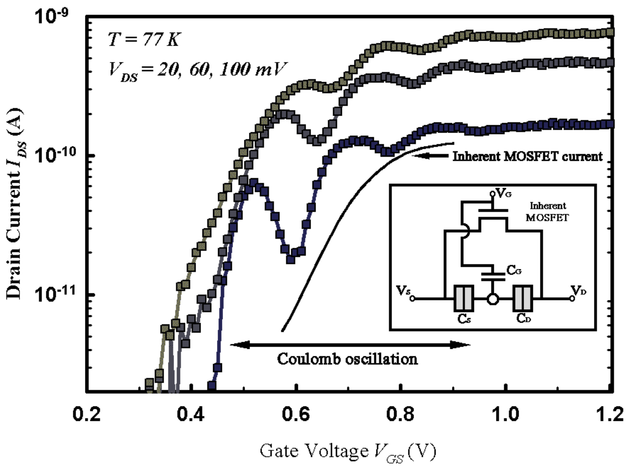

Fig. 2. Electrical characteristics of the fabricated MOSETs at 77 K. Inset shows the equivalent circuit diagram of a MOSET.

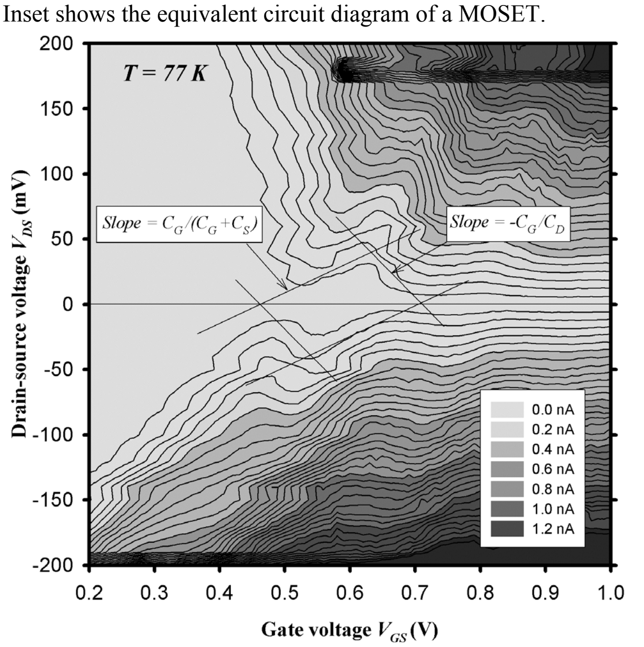

Fig. 3. Contour plot of drain current as a function of V_{GS} and V_{DS} at 77 K.

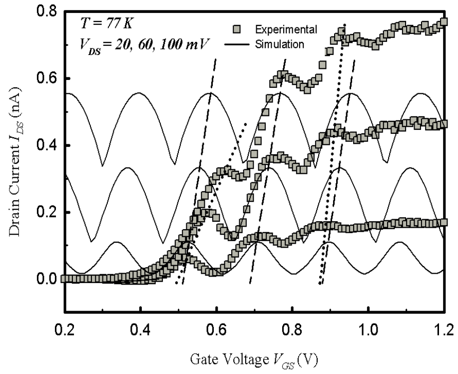

Fig. 4. SPICE Simulation results of Intrinsic SET current $I_{i\text{-}SET}$ (T = 77 K, V_{DS} = 20, 60, 100 mV). The dash lines indicate the phase shift (ΔV_{GS}) in the simulation of $I_{i\text{-}SET}$ and the dotted lines ΔV_{GS} in the measured I-V characteristics.

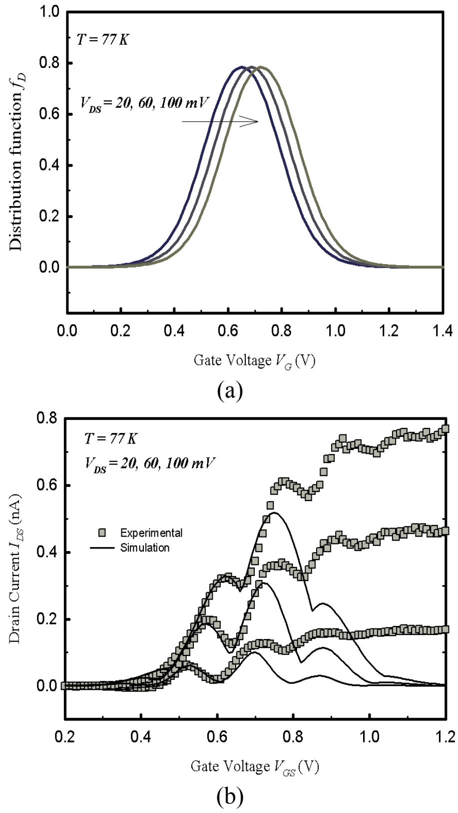

Fig. 5 (a) SPICE simulation of distribution function f_D (b) Simulation results of SET current I_{SET} using SET SPICE model with distribution function f_D (T = 77 K, V_{DS} = 20, 60, 100 mV).

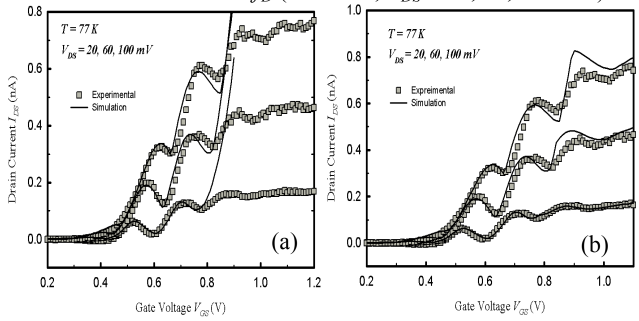

Fig. 6 (a) SPICE simulation results of MOSET current with inherent MOSFET current in subthreshold region (b) Complete SPICE simulation including linear MOSFET current region (T = 77 K, V_{DS} = 20, 60, 100 mV).